Computers & Geosciences 83 (2015) 1–16

Contents lists available at ScienceDirect

Computers & Geosciences

journal homepage: www.elsevier.com/locate/cageo

Semi-supervising Interval Type-2 Fuzzy C-Means clustering with spatial information for multi-spectral satellite image classification and change detection

Long Thanh Ngo [a,*], Dinh Sinh Mai [a], Witold Pedrycz [b,c,d]

[a] Department of Information Systems, Faculty of Information Technology, Le Quy Don Technical University, 236 Hoang Quoc Viet, Hanoi, Vietnam
[b] Department of Electrical and Computer Engineering, University of Alberta, Edmonton, AB, Canada T6R 2V4
[c] Department of Electrical and Computer Engineering, Faculty of Engineering, King Abdulaziz University Jeddah, 21589, Saudi Arabia
[d] Systems Research Institute, Polish Academy of Sciences, Warsaw, Poland

A R T I C L E I N F O

Article history:
Received 18 December 2014
Received in revised form
4 May 2015
Accepted 16 June 2015
Available online 23 June 2015

Keywords:
Interval type-2 fuzzy sets
Fuzzy C-Means
Type-2 fuzzy clustering
Satellite image analysis
Land cover classification
Change detection

A B S T R A C T

Data clustering has been widely applied to numerous real-world problems such as natural resource management, urban planning, and satellite image analysis. Especially, fuzzy clustering with its ability of handling uncertainty has been developed for image segmentation or image analysis e.g. in health image analysis, satellite image classification. Normally, image segmentation algorithms like fuzzy clustering use spatial information along with the color information to improve the cluster quality. This paper introduces an approach, which exploits local spatial information between the pixel and its neighbors to compute the membership degree by using an interval type-2 fuzzy clustering algorithm, called IIT2-FCM. Besides, a Semi-supervising Interval Type-2 Fuzzy C-Means algorithm using spatial information, called SIIT2-FCM, is proposed to move the prototype of clusters to the expected centroids which are pre-defined on a basis of available samples. The proposed algorithms are applied to the problems of satellite image analysis consisting of land cover classification and change detection. Experimental results are reported for various datasets of the LandSat7 imagery at multi-temporal points and compared with the results produced by some existing algorithms and obtained from some survey data. The clustering results assessed with regard to some validity indexes demonstrate that the proposed algorithms form clusters of better quality and higher accuracy in problems of land cover classification and change detection.

1. Introduction

In clustering-based image segmentation approaches, the most important problem is to establish a method to determine whether or not the considered pixel belongs to a certain cluster. The "conventional" clustering algorithms like k-Means, Fuzzy C-Means (FCM), and interval type-2 Fuzzy C-Means (IT2-FCM) exhibit the same strategy based on the Euclidean distance to compute the degree of similarity between objects to be assigned to clusters with the corresponding membership degree. Not only color based similarity of the pixels but also the spatial relationship between pixels and their neighbors certainly impact the clustering results.

Satellite image analysis methods based on statistical parameters have been widely used because of their easy implementation and accuracy. However, these methods are often quite expensive, time consuming and only applicable to small areas. Currently, there are several approaches to classify satellite imagery in which fuzzy logic have been widely applied because of its advantages in handling ambiguous data. Normally, satellite imagery are affected by noise because of weather and errors associated with the photographic equipment and in this case fuzzy clustering becomes of interest.

Type-2 fuzzy sets form an extension of original fuzzy sets of type-1. They have been developed and applied to various problems (Karnik et al., 1999; Karnik and Mendel, 2001; Liang and Mendel, 2000; Mendel and John, 2002; Mendel et al., 2006; Liu, 2008; Ngo and Nguyen, 2012; Nguyen et al., 2015; Hwang and Rhee, 2007; Fisher, 2010) including data clustering. Fuzzy C-Means (FCM) clustering (Bezdek et al., 1984) and its variants have been widely applied to many problems including satellite image analysis. The drawback of the FCM algorithms is the limitation in handling uncertainty. Hence, the use of interval type-2 fuzzy sets in data clustering as the interval Type-2 Fuzzy C-Means clustering algorithm (IT2FCM) was studied in Hwang and Rhee (2007). In this method, the FOU (footprint of uncertainty) of the type-2 fuzzy set

* Corresponding author.
E-mail addresses: ngotlong@mta.edu.vn (L.T. Ngo), maidinhsinh@gmail.com (D.S. Mai), wpedrycz@ualberta.ca (W. Pedrycz).

http://dx.doi.org/10.1016/j.cageo.2015.06.011
0098-3004/

is built by using two values of the fuzzifier (fuzzification coefficient) being one of the essential parameters of the FCM algorithm. Besides, in order to improve the quality of clustering in image segmentation including satellite images, various ways of using spatial information together with color information have been developed. Remote sensing image analysis is studied using various approaches exploiting fuzzy logic (Fisher, 2010; Stavrakoudis et al., 2011; Shankar et al., 2011; Liu et al., 2013; Ghaffarian and Ghaffarian, 2014; Martinez and Martinez, 2014).

The paper deals with a novel type-2 fuzzy clustering approach to the problems of land cover classification and change detection. Three essential issues are addressed in this paper:

(1) the use of local spatial information between the pixel and its neighbors to compute the membership degree in interval type-2 fuzzy clustering algorithm, called IIT2-FCM;
(2) development of the semi-supervised interval type-2 Fuzzy C-Means algorithm using spatial information, called SIIT2-FCM, with intent to navigate the prototype of clusters to the expected centroids which are pre-defined on the basis of existing samples;
(3) application of IIT2-FCM and SIIT2-FCM to the problems of land cover classification and change detection of multi-temporal points in multi-spectral remote sensing imagery.

Experimental results are reported on various datasets of Landsat7 images at multi-temporal points. A comparative analysis is provided involving results produced by some existing algorithms available in the literature. Our interest is to quantify the quality of clustering results in terms of well-known validity indexes and look at the evaluation of the clusters in terms of accuracy in land cover classification and change detection.

The paper is organized as follows: Section 2 presents a literature review on interval type-2 fuzzy clustering, spatial information and satellite analysis. Section 3 covers a background material by looking at type-2 fuzzy sets and interval type-2 C-Means clustering; Section 4 introduces spatial information, IT2-FCM with spatial information, semi-supervising IT2FCM with spatial information; while Section 5 demonstrates how to apply IIT2FCM, SIIT2FCM to land-cover classification and change detection. Section 6 covers conclusions and identifies some future works.

2. Literature review

Let us note that the main issues studied in this paper are as follows: (1) how to use interval type-2 fuzzy sets and exploit their ability of handling uncertainty better in satellite image analysis; (2) how to use spatial information together with color information in clustering algorithms; and (3) how to apply the method to satellite image analysis (land cover classification and change detection).

In what follows, we briefly review some related studies.

Some linkages with the use of type-2 fuzzy sets to clustering algorithms, applications have been identified. Ji et al. (2014) proposed interval-valued possibilistic FCM clustering to incorporate interval type-2 sets into the possibilistic FCM to better handle and manage the uncertainty implied by data. Qiu et al. (2013) introduced the modified interval type-2 FCM using spatial information to handle uncertainty in MR images. Torshizi and Zarandi (2014a, 2014b) proposed an algorithm of general type-2 fuzzy clustering for analyzing gene expression data with newly developed general type-2 cluster validity index. Zarinbal et al. (2014) proposed Interval Type-2 Relative Entropy FCM in which the uncertainty associated with membership functions is the main concern and an application to MR image segmentation was discussed. The combination of IT2FCM and other techniques such as multiple kernel technique was also proposed (Nguyen et al., 2015). These methods handle uncertainties and deal with the input features coming from multiple sources.

With regard to satellite image classification, various applications of type-2 fuzzy sets related to satellite image analysis were introduced, consisting of land cover classification (Ngo and Nguyen, 2012; Fisher, 2010). Fisher (2010) proposed remote sensing of land cover classes given that type 2 fuzzy sets reveal uncertainty, and allows the analysis to be specific about minimum, maximum, and average degree of land cover types. Multi-spectral satellite images contain uncertainty. For instance, each pixel is captured from a square depending on the resolution of image (maybe 30×30 m) which may exhibit several land covers (water, soil or vegetable). The other uncertainty could come as a result of error of equipment or software used of processing data. Hence, clustering algorithms using type-2 fuzzy sets are suitable to deal with satellite image classification.

In order to improve the quality of clustering in image segmentation including satellite images, various ways of using spatial information together with color information in FCM algorithm were proposed (Despotovic et al., 2010; Wang et al., 2009, 2013; Zhao et al., 2011, 2013; Liu and Pham, 2012; Liu et al., 2012; Zhao, 2013; Vargas et al., 2013; Benaichouche et al., 2013). Despotovic et al. (2010) used a mask whose center is the considered pixel, while relationships between pixels in the mask and the center are used to determine the degree of similarity being used to estimate the membership values. Wang et al. (2009) proposed adaptive spatial information-theoretic clustering (ASIC) algorithm with the modified objective function which exhibits a new dissimilarity measure and the weighting factor for neighborhood effect becomes fully adaptive to the image content. The ASIC enhances the smoothness towards piecewise-homogeneous segmentation and reduces the edge blurring effect. Zhao et al. (2011) and Zhao (2013) proposed two novel fuzzy clustering algorithms using the self-tuning non-local spatial information. In the first algorithm, the self-tuning non-local spatial information for each pixel is defined and then introduced into the objective function of FCM. In the second one, a novel gray level histogram is constructed by using the self-tuning non-local spatial information for each pixel, and then clustering is performed on a basis of this gray level histogram. Zhao et al. (2013) also included spatial information in the objective function of a certain generalized Fuzzy C-Means clustering algorithm, and then the kernel induced distance is adopted to substitute the Euclidean distance in the new objective function. Liu and Pham (2012) presented a fuzzy clustering algorithm which can handle spatial constraints, which is based on the notions of hyperplanes, Fuzzy C-Means, and spatial constraints. By adding a spatial regularizer into the fuzzy hyperplane based objective function, the proposed method can take into account additional important information of inherently spatial data. Liu et al. (2012) have come up with a novel fuzzy spectral clustering algorithm with robust spatial information for image segmentation (FSCRS). The similarity matrix was obtained by using a robust gray-based fuzzy similarity measure. The spectral graph partitioning method can be applied to the similarity matrix to group the gray values of the new generated image and then the corresponding pixels in the image are reclassified to obtain the final segmentation result. Vargas et al. (2013) introduced two enhanced Fuzzy C-Means clustering algorithms with spatial constraints for noisy color image segmentation. The Rank M-type L (RM-L) and L-estimators of spatial information of the pixels are involved in the FCM algorithm to provide robustness to the segmentation schemes. Wang et al. (2013) proposed an adaptive spatial information-theoretic fuzzy clustering algorithm to improve the robustness of the conventional Fuzzy C-Means (FCM) clustering algorithms for image segmentation through the incorporation of information-theoretic framework into the FCM algorithms. Benaichouche et al. (2013) proposed an improved FCM by using three phases consisting of PSO initialization, the integration of the spatial gray-level information of the image in the clustering segmentation process and the use of Mahalanobis distance to reduce the influence of the geometrical shape of data belong to different classes, and refining the segmentation results by correcting the errors of clustering by reallocating potentially misclassified pixels.

Remote sensing image analysis consisting of land cover classification and change detection is studied using various approaches in which fuzzy logic has been applied (Fisher, 2010; Stavrakoudis et al., 2011; Shankar et al., 2011; Liu et al., 2013; Ghaffarian and Ghaffarian, 2014; Martinez and Martinez, 2014) because of ability of handling ambiguous data appearing in image data due to weather conditions or the sensors. Fisher (2010) presented modelling land cover as a type-2 fuzzy set recognizing the existence of higher order vagueness. The consideration of type-2 fuzzy sets reveals the depth of the uncertainty, and allows the analyst to be specific about minimum, maximum, and average extents of land cover types and even to report fuzzy area itself as a fuzzy number and to justify descriptive qualifications of the results. Stavrakoudis et al. (2011) proposed a Boosted Genetic Fuzzy Classifier (BGFC) for land cover classification from multispectral images in which fuzzy rules are generated in an iterative fashion, incrementally covering subspaces of the feature space, as directed by a boosting algorithm. A genetic tuning stage is employed, aiming at improving the cooperation among the fuzzy rules, thus increasing the classification performance attained after the first stage. Shankar et al. (2011) proposed a wavelet feature-based supervised scheme for fuzzy classification of land covers in the framework of wavelet-fuzzy hybridization. The wavelet features obtained from wavelet transform on an image provide spatial and spectral characteristics of pixels and hence can be utilized effectively for improving accuracy in classification, instead of using original spectral features. Liu et al. (2013) proposed a novel semi-supervised SVM model using self-training approach for remote sensing land cover classification. The self-adaptive mutation particle swarm optimization algorithm was introduced to produce the optimal parameters, and the GustafsonKessel fuzzy clustering algorithm was used for the selection of unlabeled points to reduce the impact of ineffective labels. Ghaffarian and Ghaffarian (2014) proposed an Automatic Histogram-based Fuzzy C-Means (AHFCM) algorithm consisting of two steps: clustering each band of a multispectral image by calculating the slope for each point of the histogram, in two directions, and executing the FCM clustering algorithm based on specific rules, then, automatic fusion of labeled images is used to initialize and determine the number of clusters in the FCM algorithm. Martinez and Martinez (2014) introduced the technique that uses unsupervised learning and automatically determines land uses in urban areas by using spectral clustering of geographical regions with similar tweeting activity patterns.

On the basis of land cover classification, change detection is widely one of the applications to monitor the change of land covers at multi-temporal points according to various approaches (Ghosh et al., 2011; Mishra et al., 2012; Roy et al., 2014; Ghosha et al., 2014; Yuan et al., 2015). Based on fuzzy clustering, Ghosh et al. (2011) used spatial correlation between neighboring pixels of the difference image produced by comparing two images acquired on the same geographical area at different times, called unsupervised change detection. Mishra et al. (2012) proposed the technique for incorporation of local information and used hybridization algorithm of Fuzzy C-Means clustering and GustafsonKessel clustering. Further, an approach using ensemble of semi-supervised classifiers was proposed for change detection in remotely sensed images (Roy et al., 2014) by using a multiple classifier system in semi-supervised (learning) framework instead of a single weak classifier. In the manner of semi-supervised change detection, Yuan et al. (2015) proposed a new distance metric learning framework for areas change detection by abundant spectral information of hyper-spectral image in noisy condition; Liu et al. (2013) proposed a novel semi-supervised SVM model using self-training approach to address the problem of remote sensing land cover classification.

3. Background

3.1. Type-2 fuzzy sets

A type-2 fuzzy set in X is denoted by $\tilde{A}$, and its membership grade of $x \in X$ is $\mu_{\tilde{A}}(x, u)$, $u \in J_x \subseteq [0, 1]$, which is a type-1 fuzzy set in [0, 1]. The set of $J_x\,(x \in X)$ is called primary memberships of x in $\tilde{A}$ and memberships of primary memberships in $\mu_{\tilde{A}}(x, u)$ are called secondary memberships of x in $\tilde{A}$.

Definition 3.1. A type-2fuzzy set, denoted $\tilde{A}$, is characterized by a type-2 membership function $\mu_{\tilde{A}}(x, u)$ where $x \in X$ and $u \in [0, 1]$ i.e.

$$\tilde{A} = \{((x, u), \mu_{\tilde{A}}(x, u))|x \in X, u \in [0, 1]\} \tag{1}$$

or

$$\tilde{A} = \int_{x \in X} \int_{u \in [0,1]} \mu_{\tilde{A}}(x, u))/(x, u) \tag{2}$$

in which $0 \le \mu_{\tilde{A}}(x, u) \le 1$.

At each value of x, say $x = x'$, the 2-D plane whose axes are u and $\mu_{\tilde{A}}(x', u)$ is called a *vertical slice* of $\mu_{\tilde{A}}(x, u)$. A *secondary membership function* is a vertical slice of $\mu_{\tilde{A}}(x, u)$. It is $\mu_{\tilde{A}}(x = x', u)$ for $x \in X$ and $\forall\, u \in [0, 1]$ i.e.

$$\mu_{\tilde{A}}(x = x', u) \equiv \mu_{\tilde{A}}(x') = \int_{u \in [0,1]} f_{x'}(u)/u \tag{3}$$

in which $0 \le f_{x'}(u) \le 1$.

Type-2 fuzzy sets are called an interval type-2 fuzzy sets if the secondary membership function $f_{x'}(u) = 1$, $u \in [0, 1]$ i.e. a type-2 fuzzy set are defined as follows:

Definition 3.2. An interval type-2 fuzzy set $\tilde{A}$ is characterized by an interval type-2 membership function $\mu_{\tilde{A}}(x, u) = 1$ where $x \in X$ and $u \in [0, 1]$ i.e.

$$\tilde{A} = \{((x, u), 1)|x \in X, u \in [0, 1]\} \tag{4}$$

Uncertainty of $\tilde{A}$, denoted FOU, is union of primary functions i.e. $FOU(\tilde{A}) = \bigcup_{x \in X} J_x$. Upper/lower bounds of membership function (UMF/LMF), denoted $\overline{\mu}_{\tilde{A}}(x)$ and $\underline{\mu}_{\tilde{A}}(x)$, of $\tilde{A}$ are two type-1 membership function and bounds of FOU.

3.2. Interval type-2 Fuzzy C-Means algorithm

In general, fuzzy membership functions in interval type-2 Fuzzy C-Means algorithm (Hwang and Rhee, 2007) are construction by computing the relative distance among the patterns and cluster centroids. Hence, to define the interval of primary membership for a pattern, we define the lower and upper interval memberships using two different values of m. In (6) and (7), m_1 and m_2 are different values of the fuzzifiers. The interval of a primary membership is defined for a pattern, as the highest and lowest primary membership for a pattern. These values are upper and lower membership grades of a pattern, respectively.

IT2FCM form an extension of the FCM by using two fuzziness parameters m_1 and m_2 to build FOU, corresponding to upper and lower values of fuzzy clustering. The use of these fuzzifiers results in different objective functions to be minimized:

$$\begin{cases} J_{m_1}(U, v) = \sum_{k=1}^{N}\sum_{i=1}^{C}(u_{ik})^{m_1} d_{ik}^2 \\ J_{m_2}(U, v) = \sum_{k=1}^{N}\sum_{i=1}^{C}(u_{ik})^{m_2} d_{ik}^2 \end{cases} \tag{5}$$

in which $d_{ik} = \|x_k - v_i\|$ is the Euclidean distance between the pattern x_k and the centroid v_i, C is the number of clusters and N is the number of patterns, and u_{ik} is the membership degree of x_k belonging to cluster i with an interval $\underline{u}_{ik}$ and $\overline{u}_{ik}$ which are determined as follows:

$$\overline{u}_{ik} = \begin{cases} \dfrac{1}{\sum_{j=1}^{C}\left(\dfrac{d_{ik}}{d_{jk}}\right)^{2/(m_1-1)}} & \text{if } \dfrac{1}{\sum_{j=1}^{C}\left(\frac{d_{ik}}{d_{jk}}\right)} < \dfrac{1}{C} \\ \dfrac{1}{\sum_{j=1}^{C}\left(\dfrac{d_{ik}}{d_{jk}}\right)^{2/(m_2-1)}} & \text{otherwise} \end{cases} \tag{6}$$

$$\underline{u}_{ik} = \begin{cases} \dfrac{1}{\sum_{j=1}^{C}\left(\dfrac{d_{ik}}{d_{jk}}\right)^{2/(m_1-1)}} & \text{if } \dfrac{1}{\sum_{j=1}^{C}\left(\frac{d_{ik}}{d_{jk}}\right)} \ge \dfrac{1}{C} \\ \dfrac{1}{\sum_{j=1}^{C}\left(\dfrac{d_{ik}}{d_{jk}}\right)^{2/(m_2-1)}} & \text{otherwise} \end{cases} \tag{7}$$

in which $i = 1, \ldots, C$ and $k = 1, \ldots, N$.

Because each pattern comes with a membership interval as the bounds: the upper $\overline{u}$ and the lower $\underline{u}$, each centroid of cluster is represented by the interval between v^L and v^R. Cluster centroids are computed in the same way as in the standard FCM that is

$$v_i = \frac{\sum_{k=1}^{N}(u_{ik})^m x_k}{\sum_{k=1}^{N}(u_{ik})^m} \tag{8}$$

$i = \overline{1, C}$.

After determining v_i^R, v_i^L using the KM algorithm (Karnik and Mendel, 2001), type-reduction is applied to form centroids of the clusters:

$$v_i = \frac{v_i^R + v_i^L}{2} \tag{9}$$

For membership grades, we have

$$u_{ij} = \frac{u_{ij}^R + u_{ij}^L}{2}, \quad i = 1, \ldots, C, \; j = 1, \ldots, N \tag{10}$$

In which, $u_{ij}{}^L$ and $u_{ij}{}^R$ are determined as follows:

$$u_{ij}^L = \sum_{l=1}^{M} u_{ij}^l / M \quad \text{where } u_{ij}^l = \begin{cases} \overline{u}_{ij} & \text{if } x_{il} \text{ uses } \overline{u}_{ij} \text{ for } v_i^L \\ \underline{u}_{ij} & \text{otherwise} \end{cases} \tag{11}$$

$$u_{ij}^R = \sum_{l=1}^{M} u_{ij}^l / M \quad \text{where } u_{ij}^l = \begin{cases} \overline{u}_{ij} & \text{if } x_{il} \text{ uses } \overline{u}_{ij} \text{ for } v_i^R \\ \underline{u}_{ij} & \text{otherwise} \end{cases} \tag{12}$$

in which M is the number of features of patterns.

Next, the defuzzification for IT2-FCM is completed: if $u_{ik} > u_{jk}$ for $j = 1, \ldots, C$ and $i \ne j$ then x_k is assigned to cluster i.

4. Semi-supervising Interval Type-2 Fuzzy C-Means clustering with spatial information

4.1. Spatial information

In fact, image information is stored as a set of numeric values, image partitions are usually based on the degree of similarity among these values to decide whether an object belongs to any region in the image. Therefore, the key to determine a pixel belonging to certain area is based on the similarity of these colors, which is calculated through a distance function in the color space $d_{ik} = \|x_k - v_i\|$ e.g. Euclidean distance between the pattern x_k and the centroid v_i.

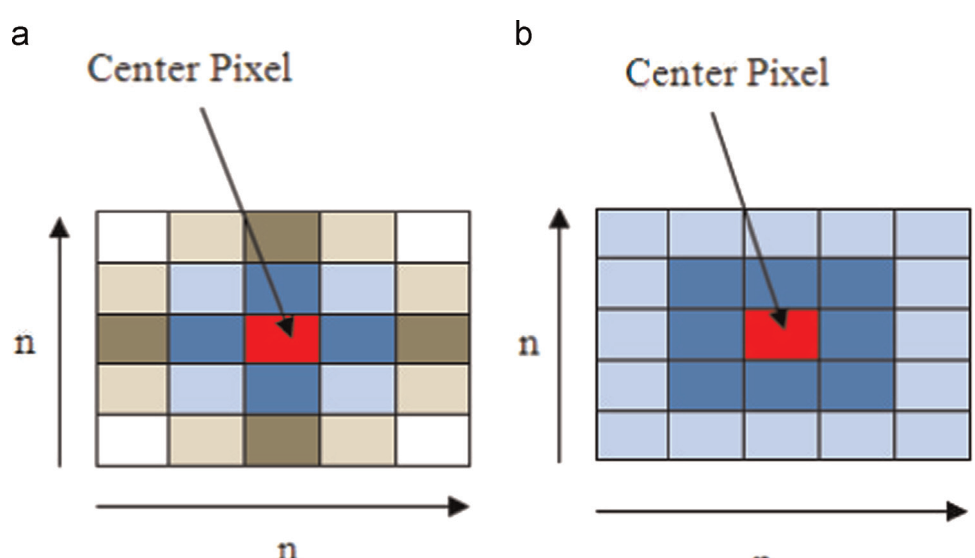

Fig. 1. The masks describing the relationship space between the center pixel and neighboring pixels: (a) 4-directional mask and (b) 8-directional mask.

We use a mask of size $n \times n$ to position on the image, the center pixel of mask is the considered pixel. The number of neighboring pixels is determined corresponding to the selected type of mask i.e. 8 pixels for the 8-directional mask or 4 pixels for the 4-directional mask, which are shown in Fig. 1. Fig. 1(a) shows the case of 4-directional mask in which if $n=2$, there are 4 neighboring pixels; if $n=3$, there are 12 neighboring pixels involving 4 neighboring pixels of the center pixel and their neighboring pixels according to 4-directional mask. In the same way, Fig. 1(b) shows the case of 8-directional mask in which if $n=2$, there are 8 neighboring pixels; if $n=3$, there are 24 neighboring pixels.

To determine the degree of influence of the neighboring pixels for the center pixels, a spatial information measure SI_{ik} is defined on the basis of the degree u_{ki} and the attraction distance d_{ki}:

$$SI_{ik} = \frac{\sum_{j=1}^{N} u_{ij} d_{kj}^{-1}}{\sum_{j=1}^{N} d_{kj}^{-1}} \tag{13}$$

in which u_{ij} is the membership degree of the neighboring element x_j to the cluster i. The distance attraction d_{kj} is the squared Euclidean distance between elements (x_k, y_k) and (x_j, y_j). According to the above expression, spatial information of each pixel comes with the higher value if its color is the similar as color of neighboring pixels and vice versa. We use the inverse distance d_{kj}^{-1} because the closer neighbors x_j of the center x_k are the more influence they exert on the result and vice versa. Fig. 1 illustrates the neighborhood configuration used in this work.

For the proposed fuzzy clustering a new distance is defined as follows:

$$R_{ik} = \|x_k - v_i\|^2 (1 - \alpha e^{-SI_{ik}}) \tag{14}$$

where S_{ij} is the spatial relationship information between elements x_k and clusters i, $\alpha \in [0, 1]$ is the parameter that controls the relative impact of neighboring pixels. If $\alpha=0$, R_{ik} is the squared Euclidean distance and the algorithm reduces to the original standard FCM.

The idea behind the use of this spatial relationship information can be outlined as follows: consider the local $n \times n$ mask in which intensity differences between the center x_k and the closest neighboring pixels x_k are large and the one has similar intensity as the cluster centroid v_i. If the neighborhood attraction, SI_{ij}, takes a large value then the expression $(1 - \alpha e^{-SI_{ik}})$ will assume a small value for all $\alpha \neq 0$. After each iteration of the algorithm, the central element x_k will be attracted to the cluster i. If the neighborhood attraction SI_{ik} continuously takes on a large value until the algorithm terminates then the central element x_k will be assigned to the cluster i.

4.2. Interval Type-2 Fuzzy C-Means clustering with spatial information (IIT2-FCM)

The main idea behind the IIT2-FCM algorithm is extended from IT2-FCM by adding the spatial information to calculate distance between clusters and pixels. The diagram of the proposed algorithm is described in Fig. 2. The ensuing steps are described as follows:

Initialization of matrix centroid V.

Secondly, the primary memberships $\bar{u}_{ik}$ and $\underline{u}_{ik}$ for a pattern are corresponding to two fuzzifiers m_1 and m_2 whose values were chosen arbitrarily.

Then the value of spatial information of each pixels SI_{ik} is computed as the following formulas. Because each pattern comes from the membership interval between $\bar{u}$ and $\underline{u}$, with the upper bound $\bar{u}$ and the lower bound $\underline{u}$, SI_{ij} is an interval with two bounds which are computed corresponding to the upper and lower

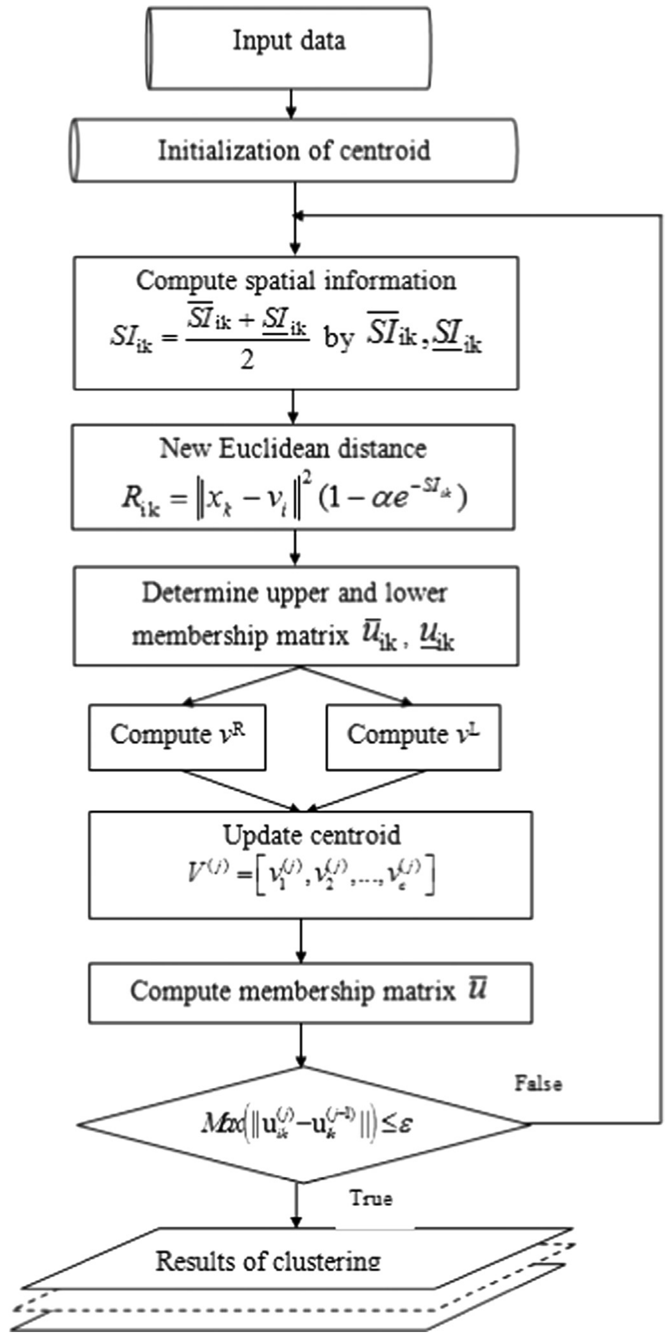

Fig. 2. Diagram of IIT2FCM using spatial information.

membership values:

$$\overline{SI}_{ik} = \frac{\sum_{j=1}^{N} \bar{u}_{ij} (d_{kj})^{-1}}{\sum_{j=1}^{N} (d_{kj})^{-1}} \tag{15}$$

$$\underline{SI}_{ik} = \frac{\sum_{j=1}^{N} \underline{u}_{ij} (d_{kj})^{-1}}{\sum_{j=1}^{N} (d_{kj})^{-1}} \tag{16}$$

Then the value of the spatial information is defuzzified as

$$SI_{ik} = (\overline{SI}_{ik} + \underline{SI}_{ik})/2 \tag{17}$$

We compute the distance in the form

$$R_{ik} = \|x_k - v_i\|^2 (1 - \alpha e^{-SI_{ik}}) \tag{18}$$

We define a set $I_k = \{i|1 \le i \le C, R_{ik} = 0\}$ in which $k = 1, \ldots, N$ and $\|x_k - v_i\|$ is the Euclidean distance between data sample k and cluster i in M-dimensional space. In case of $I_k = \emptyset$, $\overline{u}_{ik}$ and $\underline{u}_{ik}$ are determined in the same way by using (6) and (7) and replacing the distance d_{ij} by the new distance R_{ij}:

$$\overline{u}_{ik} = \begin{cases} \dfrac{1}{\sum_{j=1}^{C} (R_{ik}/R_{jk})^{2/(m_1-1)}} & \text{if } \dfrac{1}{\sum_{j=1}^{C} (R_{ik}/R_{jk})} < \dfrac{1}{C} \\ \dfrac{1}{\sum_{j=1}^{C} (R_{ik}/R_{jk})^{2/(m_2-1)}} & \text{if } \dfrac{1}{\sum_{j=1}^{C} (R_{ik}/R_{jk})} \ge \dfrac{1}{C} \end{cases} \tag{19}$$

$$\underline{u}_{ik} = \begin{cases} \dfrac{1}{\sum_{j=1}^{C} (R_{ik}/R_{jk})^{2/(m_1-1)}} & \text{if } \dfrac{1}{\sum_{j=1}^{C} (R_{ik}/R_{jk})} \ge \dfrac{1}{C} \\ \dfrac{1}{\sum_{j=1}^{C} (R_{ik}/R_{jk})^{2/(m_2-1)}} & \text{if } \dfrac{1}{\sum_{j=1}^{C} (R_{ik}/R_{jk})} < \dfrac{1}{C} \end{cases} \tag{20}$$

Otherwise, if $I_k \neq \emptyset$, $\overline{u}_{ik}$ and $\underline{u}_{ik}$ are determined in the form

$$\overline{u}_{ik} = \begin{cases} 0 & \text{if } i \notin I_k \\ \sum_{i \in I_k} \overline{u}_{ik} = 1 & \text{if } i \in I_k \end{cases} \tag{21}$$

$$\underline{u}_{ik} = \begin{cases} 0 & \text{if } i \notin I_k \\ \sum_{i \in I_k} \underline{u}_{ik} = 1 & \text{if } i \in I_k \end{cases} \tag{22}$$

in which $i = 1, \ldots, C$, $k = 1, \ldots, N$.

Because each pattern is described by the membership interval $\overline{u}$ and $\underline{u}$, therefore each centroid of the cluster is represented by the interval localized in between v^L and v^R. To determine v^L and v^R, we apply the KM algorithm (Karnik and Mendel, 2001) as follows:

Algorithm 1. Determine v^L (or v^R).

Step 1: Calculate $\overline{u}_{ij}$, $\underline{u}_{ij}$ with the use (19) and (20).

Step 2: Set a value of m, $m \ge 1$;

Compute $v'_j = (v'_{j1}, \ldots, v'_{jM})$ with the aid of (8) and $u_{ij} = \frac{(\overline{u}_{ij} + \underline{u}_{ij})}{2}$.

Sort N patterns for each of M features in ascending order.

Step 3: Find index k such that $x_{kl} \le v'_{jl} \le x_{(k+1)l}$ with $1 \le k \le N$ and $l = 1, \ldots, M$.

Step 4: Calculate v'' as follows:

In the case of computing v^L:

$$v'' = \frac{\sum_{l=1}^{k} x_l \overline{u}_{il} + \sum_{l=k+1}^{N} x_l \underline{u}_{il}}{\sum_{l=1}^{k} \overline{u}_{il} + \sum_{l=k+1}^{N} \underline{u}_{il}} \tag{23}$$

In the case of computing v^R:

$$v'' = \frac{\sum_{l=1}^{k} x_l \underline{u}_{il} + \sum_{l=k+1}^{N} x_l \overline{u}_{il}}{\sum_{l=1}^{k} \underline{u}_{il} + \sum_{l=k+1}^{N} \overline{u}_{il}} \tag{24}$$

Step 5: If $v' = v''$ go to Step 6

else

Set $v' = v''$

Back to Step 3.

Step 6: Set $v^L = v'$ (or $v^R = v'$).

After obtaining v^R, v^L, form the centroids of the clusters using (9).

For membership grades u_{ik} follow (10)–(12).

Next, the defuzzification is realized in the form: if $u_{ik} > u_{jk}$ for $j = 1, \ldots, C$ and $i != j$ then x_k is assigned to cluster i.

Algorithm 2. IIT2-FCM algorithm.

Step 1: Initialization

1.1. Selection of the values of the parameters m_1, m_2 $(1 < m_1, m_2)$, termination criterion value ε.

1.2. Initialization of centroids $V = [v_i]$, $v_i \in R^M$, $i = 1, \ldots, C$.

Step 2: Compute the fuzzy partition matrix $\overline{u}$, $\underline{u}$ and update centroids V:

2.1. Calculate the value of spatial information SI_{ik} by using (15)–(17).

2.2. Calculate the upper/lower membership degree matrix $\overline{u}_{ik}$, $\underline{u}_{ik}$ using (19)–(22).

2.3. Update the centroids of clusters $V^j = [v_1^j, v_2^j, \ldots, v_C^j]$ by finding v^L and v^R (Algorithm 1) and (8).

2.4. Calculate the membership degree matrix u_{ik} using (10)–(12).

Step 3: Verify if the termination condition is satisfied:

If Max $|u_{ik}^{(j)} - u_{ik}^{(j-1)}| < \varepsilon$ go to step 4, otherwise go to step 2.

Step 4:

4.1. Assign a pattern to a cluster.

4.2. Report results of clustering.

It is known that the computational complexity of FCM, k-Means algorithm is $O(nCM)$, and IT2-FCM is $O(n^2C^2M)$ where M is the dimensionality of the data points.

Meanwhile, each iteration of the IIT-2FCM algorithm has to compute spatial relationship information of each pixel, the computational complexity is $O(n^2)$. Moreover, these calculations are not affected by the number of data dimensions and the number of clusters, thus, the computational complexity of IIT2-FCM as well as the complexity of the IT2-FCM algorithm is $O(n^2C^2M)$.

4.3. Semi-supervising Interval Type-2 Fuzzy C-Means clustering with spatial information

Normally, fuzzy clustering algorithms determine the prototype of clusters depending on the structure of data samples i.e. individual sample could form a different set of prototypes of clusters. In fact, a family of problems always leads to the same prototypes with fixed centroids for all datasets. For example, prototype of clusters in classification problem of remote sensing images is not changed for all data samples. Hence, conventional fuzzy clustering algorithms could produce incorrect results, especially when encountering dataset in which the large differences appear in sizes of clusters. Fig. 3 visualizes the example of satellite images with the large differences between clusters, in which almost area of the region is water cluster, the areas of fields, sparse tree and planted forests, low woods are medium, whereas the areas of rocks, bare soil and jungles are very small. Because of the physical properties of electromagnetic spectrum when reflecting the land cover types, the centroid of clusters is fixed for all types of land covers.

Consider a classification problem of multi-spectral images with k-bands with dataset involving a set of pixels $P = \{p_1, \ldots, p_N\}$, N is the number of pixels, $p_i = \langle p_{i1}, \ldots, p_{ik} \rangle$, $i = 1, \ldots, N$ are component vectors corresponding to k-bands of images. Dataset P is partitioned into C clusters based on the similarity of component vectors. As mentioned above, the prototypes of clusters are fixed for all datasets of satellite images, provided that $V^* = \langle v_1^*, \ldots, v_C^* \rangle$ are

Fig. 3. The example of satellite images with the large differences between clusters.

set of centroids of clusters. The set V^* could be manually determined by taking samples coming from survey datasets in the following way:

For each cluster, we take a set of pixels $P(k) = \{p_1, \dots, p_m\}$ which exactly belong to the considered cluster. For example of water cluster, we take a set of pixels in the image that belong to water regions. The centroid of the considered cluster is the mean of component vectors i.e.

$$v_k^* = \frac{\sum_{j=1}^{m} p_j}{m} \tag{25}$$

After producing V^*, the idea behind this approach is to use the pre-defined collection of centroids V^* to adjust centroid of clusters to move closer to V^* by extending the IIT2-FCM with spatial information, called Semi-supervising Interval Type-2 Fuzzy C-Means with spatial information (SIIT2-FCM). In fact, V^* is used to adjust the centroids v_k so that the closer the computing centroid of clusters is V^*, the best data cluster i.e. the distance from the centroids and V^* appears in the objective function to minimize. Hence, V^* is as one of parameters to influence to the process of minimizing the objective function i.e. adjusting the centroids to the expected positions.

The diagram is described in Fig. 4.

Let $D_{vi} = \| v_i - v_i^* \|$ be a distance between the computed clusters and the sampled cluster. We define a new objective function:

$$J_m(U, v) = \sum_{j=1}^{N} \sum_{i=1}^{C} (u_{ij})^m [R_{ij}^2 + D_{vi}^2] \tag{26}$$

in which $\sum_{i=1}^{C} u_{ij} = 1$. In case of interval type-2 FCM, we have two objective functions as follows:

$$J_{m1}(U, v) = \sum_{j=1}^{N} \sum_{i=1}^{C} (u_{ij})^{m1} [R_{ij}^2 + D_{vi}^2] \tag{27}$$

$$J_{m2}(U, v) = \sum_{j=1}^{N} \sum_{i=1}^{C} (u_{ij})^{m2} [R_{ij}^2 + D_{vi}^2] \tag{28}$$

To minimize the objective function, the method of Lagrange multipliers is used to find the following solution:

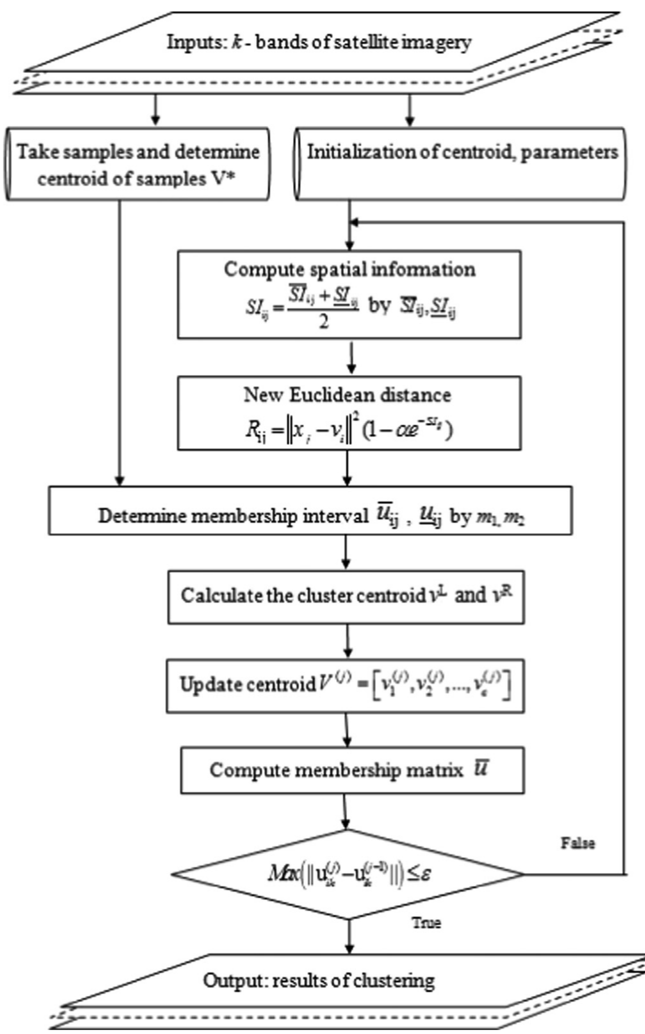

Fig. 4. Diagram of Semi-supervising Interval Type-2 Fuzzy clustering.

$$L(u_{ij}, \lambda_j) = \sum_{j=1}^{N}\sum_{i=1}^{C}(u_{ij})^m[R_{ij}^2 + D_{vi}^2] + \sum_{j=1}^{N}\lambda_j(1 - \sum_{i=1}^{C}u_{ij}) \tag{29}$$

Let $D_{ij} = R_{ij}^2 + D_{vi}^2$ and calculate the first derivative:

$$\begin{cases} \dfrac{dL}{du_{ij}} = m\cdot u_{ij}^{m-1}\cdot D_{ij} - \lambda_j = 0 \\ \dfrac{dL}{d\lambda_j} = 1 - \sum_{i=1}^{C}u_{ij} = 0 \end{cases} \tag{30}$$

$$\begin{cases} \lambda_j = \dfrac{m}{\sum_{i=1}^{C}\left[\dfrac{1}{D_{ij}}\right]^{1/(m-1)}} \\ u_{ij} = \left[\dfrac{1}{D_{ij}\sum_{i=1}^{C}\left[\dfrac{1}{D_{ij}}\right]^{1/(m-1)}}\right]^{1/(m-1)} \end{cases} \tag{31}$$

Because the algorithm uses two fuzzifiers m_1 and m_2 to construct an interval of membership grades, so we construct the membership interval as follows:

$$\bar{u}_{ik} = \begin{cases} \left[\dfrac{1}{D_{ij}\sum_{j=1}^{C}(1/D_{ij})^{1/(m1-1)}}\right]^{1/(m1-1)} & \text{if } \dfrac{1}{D_{ij}\sum_{j=1}^{C}(1/D_{ij})} < \dfrac{1}{C} \\ \left[\dfrac{1}{D_{ij}\sum_{j=1}^{C}(1/D_{ij})^{1/(m2-1)}}\right]^{1/(m2-1)} & \text{if } \dfrac{1}{D_{ij}\sum_{j=1}^{C}(1/D_{ij})} \geq \dfrac{1}{C} \end{cases} \tag{32}$$

$$\underline{u}_{ik} = \begin{cases} \left[\dfrac{1}{D_{ij}\sum_{j=1}^{C}(1/D_{ij})^{1/(m1-1)}}\right]^{1/(m1-1)} & \text{if } \dfrac{1}{D_{ij}\sum_{j=1}^{C}(1/D_{ij})} \geq \dfrac{1}{C} \\ \left[\dfrac{1}{D_{ij}\sum_{j=1}^{C}(1/D_{ij})^{1/(m2-1)}}\right]^{1/(m2-1)} & \text{if } \dfrac{1}{D_{ij}\sum_{j=1}^{C}(1/D_{ij})} < \dfrac{1}{C} \end{cases} \tag{33}$$

The primary membership interval $[\bar{u}_{ik}, \underline{u}_{ik}]$ is for a pattern with two fuzzifiers m_1 and m_2, update the centroid $V^j = [v_1^j, v_2^j, \ldots, v_c^j]$ by using algorithm for finding v^L and v^R (Algorithm 1).

Algorithm 3. The SIIT2-FCM algorithm.

Step 1: Take C individual samples
1.1. One after the other cluster, take C individual samples from multi-spectral satellite images are characterized for C clusters.
1.2. Calculating centroid $V^* = [v_i^*]$, $v_i^* \in R^M$, $i = 1, \ldots, C$ of samples by averaging points present in each sample using (25).
Step 2: Initialization
2.1. Choose values of the fuzzifiers m_1, m_2 $(1 < m_1, m_2)$, termination criterion value ε.
2.2. Initialization centroid $V = [v_i]$, $v_i \in R^n$.
Step 3: Compute the membership matrix $\overline{U}$, $\underline{U}$ and update centroid V:
3.1. Calculate the value of spatial information SI_{ik} by using (15)–(17).
3.2. Calculate the upper/lower membership degree matrix $\bar{u}_{ik}$, $\underline{u}_{ik}$ using (32) and (33).
3.3. Update the centroids of clusters $V^j = [v_1^j, v_2^j, \ldots, v_c^j]$ by finding v^L and v^R (Algorithm 1) and (8).
3.4. Calculate the membership degree matrix u_{ik} by using (10)–(12).
Step 4: Verify if the termination condition is satisfied:
If Max $|u_{ik}^{(j)} - u_{ik}^{(j-1)}| < \varepsilon$ go to step 4, otherwise go to step 2.
Step 5:
5.1. Assign a pattern to a cluster.
5.2. Report results of clustering.

5. Land-cover classification and change detection

5.1. Land-cover classification

In the ensuing experiments, land cover classification is implemented for *Landsat*7 multi-spectral satellite images with resolution of 30 m × 30 m. Because, land covers such as forestry, agriculture, bare land, and water surface usually do not clearly define boundaries, an individual pixel can comprise information about partial membership e.g. a rate of 0.30 of soil, rate of 0.25 of forest and rate of 0.45 of water. In this case, the pixel is assigned as water cover, but its rate of 0.55 is no water and applying a Boolean (yes–no) classification is neither suitable nor practically convincing. Therefore, fuzzy clustering, in which a pixel can be assigned into many layers according to the membership grades, is more suitable than Boolean clustering (Bezdek and Pal, 1998).

Multi-spectral images are one of the types which acquired from remote sensing (RS) radiometers. By dividing the spectrum into many bands, multi-spectral is the opposite of panchromatic, which only records the total intensity of radiation falling on each pixel. Usually, satellites have three or more radiometers. Each one acquires one digital image (in remote sensing, called a 'scene') in a small band of visible spectra, ranging from 400 nm to 700 nm, called red–green–blue (RGB) section, and going to infrared wavelengths of 700 nm to 1500 nm or more, classified as near infrared (NIR), middle infrared (MIR) and far infrared (FIR or thermal). In the case of *Landsat*7 image, seven scenes combine into a seven-bands multi-spectral imagery.

Type-2 fuzzy clustering algorithms exhibit the ability of handling the uncertainty or ambitious data that appears from input data of images. The IIT2-FCM or SIIT2-FCM are applied to classify land covers from *Landsat*7 imagery consisting of 7 bands numbered from 1 to 7, in which wavelength and waveband are described in Table 1. In order to increase precision of classification, we used 6 bands of *Landsat*7 images. The sixth band of *Landsat*7 images is not used because of being the thermal infrared band

Table 1
The electromagnetic spectrum of bands of the Landsat7 imagery.

Band no.	Waveband	Wavelength (nm)
1	Blue	450–520
2	Green	520–600
3	Red	630–690
4	Very near-infrared	760–900
5	Near-infrared	1550–1750
7	Shortwave infrared	2080–2350

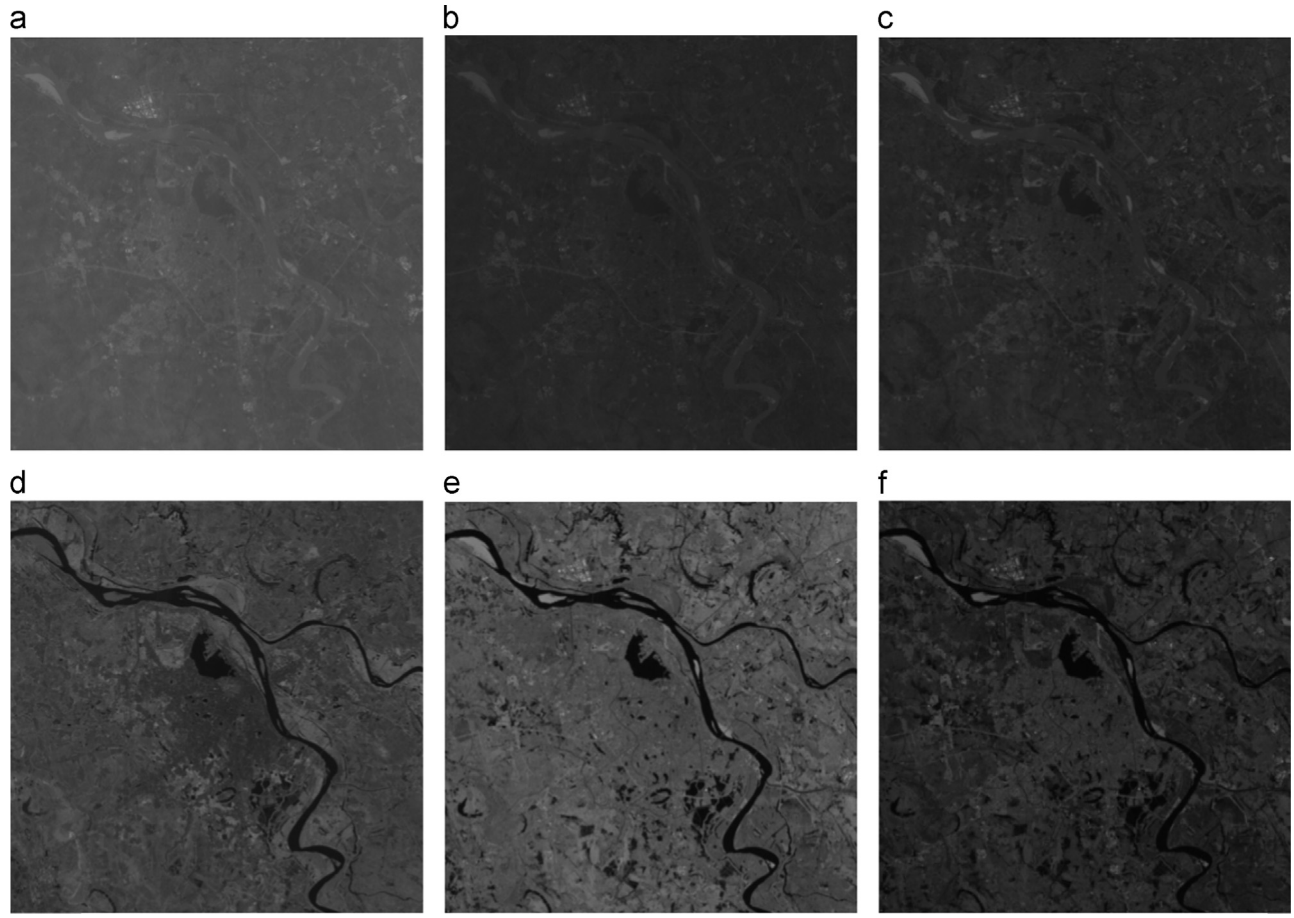

Fig. 5. Study data of Hanoi: (a) Band 1, (b) band 2, (c) band 3, (d) band 4, (e) band 5, and (f) band 7.

which is mainly used to calculate the surface temperature of the surface. Let $X = \{\mathbf{x}_1, \ldots, \mathbf{x}_N\}$, in which N is the number of pixels, $\mathbf{x}_i = (x_{i1}, x_{i2}, x_{i3}, x_{i4}, x_{i5}, x_{i7})$ is the grey level vector of image bands i.e. x_{i6} corresponding to the 6th band is not used. The clustering algorithms are used to classify X into 6 sub-sets (classes) corresponding to the 6 types of land covers as follows:

- Class 1: Rivers, ponds, lakes.
- Class 2: Rocks, bare soil.
- Class 3: Fields, sparse tree.
- Class 4: Planted forests, low woods.
- Class 5: Perennial tree crops.
- Class 6: Jungles.

The study dataset of the *Landsat*7 imagery concerns Hanoi region, Vietnam (21°54′23. 11″N, (105°03′06. 47″E to 20°55′14. 25″N, 106°02′58′. 57″E) with area of 3774.8736 km^2. The size of each image band is 2048×2048 pixels and the resolution is $30\ \text{m} \times 30\ \text{m}$ per pixel. Hence, the value of N is 4,194,304 pixels. Fig. 5 shows 6 bands of Hanoi data from band 1 to band 7, excluding band 6.

The experimental results are shown in Fig. 6 involving 6 images in which Fig. 6(a) is NDVI (Normalized Difference Vegetation Index) image generated as follows:

$$NVDI = \frac{NIR - Red}{NIR + Red} \tag{34}$$

where *Red* and *NIR* are 3 and 4 bands, respectively. Fig. 6(b), (c), (d), (e) and (f) are land cover classification of SIIT2-FCM, IIT2-FCM, IT2-FCM, FCM, and k-Means algorithms, respectively. Table 2 shows the comparison of classification results between SIIT2-FCM, IIT2-FCM, IT2-FCM, FCM and k-Means and survey data of the Vietnamese Center of Remote Sensing Technology (VCRST) which is actual data of land covers collected by land survey of individual class. In Table 2, the results of algorithms are summarized according to area of individual class and difference between the classified result and VCRST of individual class. The results show that SIIT2-FCM and IIT2-FCM obtain the better clusters for land covers with the mean and standard deviation being lower than previous algorithms. SIIT2FCM obtained classification better than IIT2FCM in which classification of classes 1, 2, 3, 4 and 6 are the best results in comparison with data of VCRST, class 5 is similar to IIT2FCM, especially, the mean and the standard deviation obtained from SIIT2FCM are significantly smaller than IIT2FCM. The percentage of difference of individual class is computed:

$$P_i = \frac{area_i - area_{i0}}{area_{i0}}. \tag{35}$$

where $area_i$ and $area_{i0}$ are the area of the ith class according to the classified results and data of VCRST, respectively.

Comparing the experimental results with the results of VCRST in Table 3, the largest difference of k-Means is 105.09%, FCM is 85.62% and IT2-FCM algorithm is 35.26%. Meanwhile, the results of SIIT2-FCM and IIT2-FCM algorithms do not exceed 3.05% and 14.38%, respectively. Fig. 6 also shows that SIIT2-FCM classifier gives clusters better. Lower accuracy of classification for class 1 may be seen in Fig. 6(c) (FCM) and Fig. 6(d) (k-Means), especially in the river region (localized at the center of the image).

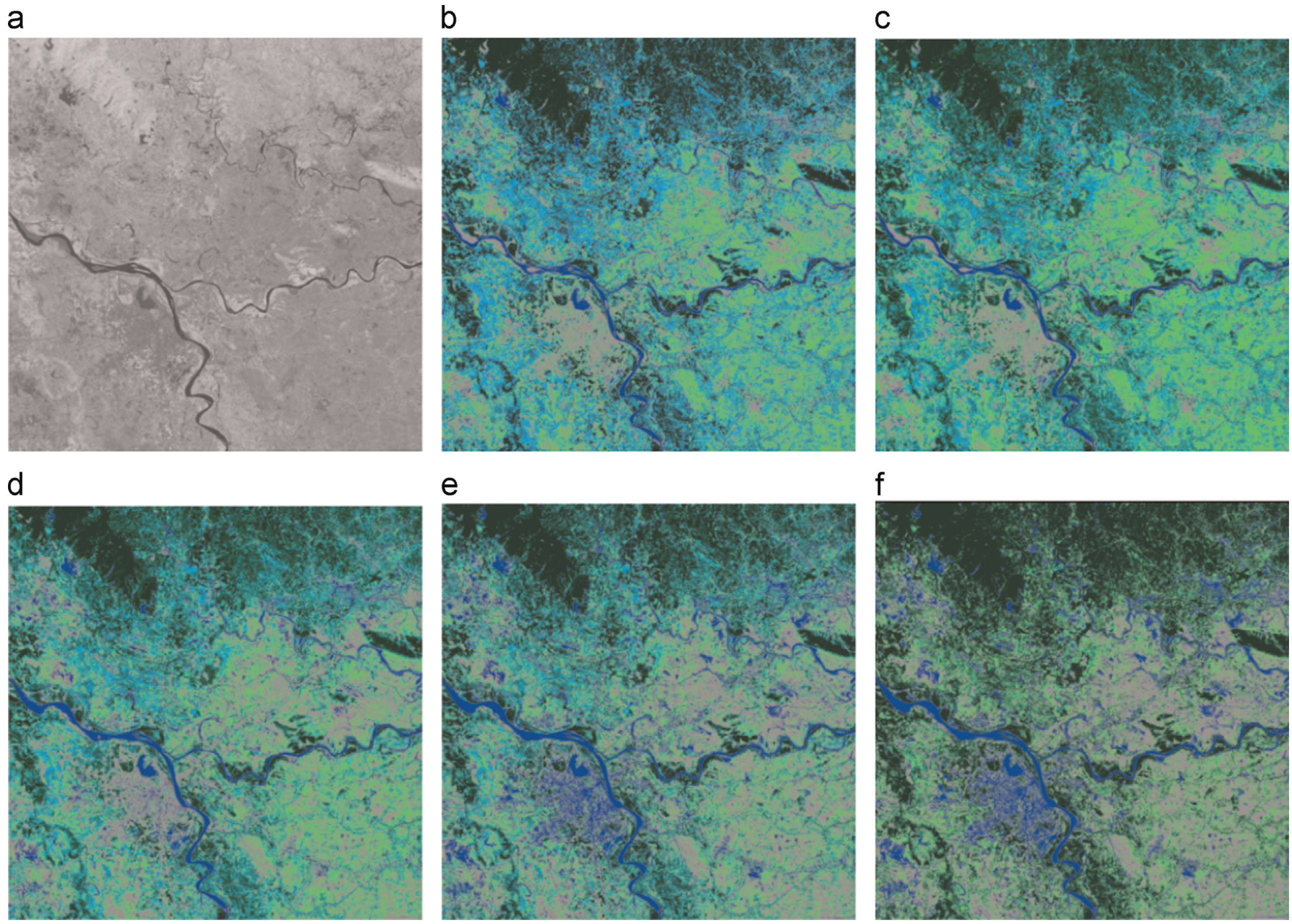

Fig. 6. Result of land cover classification. (a) NDVI, (b) SIIT2-FCM, (c) IIT2-FCM, (d) IT2-FCM, (e) FCM, and (f) *K*-Means.

Table 2
Results of land cover classification (km^2).

Class	VCRST	SIIT2-FCM		IIT2-FCM		IT2-FCM		FCM		k-Means	
	Area	Area	Diff.	Area	Diff.	Area	Diff.	Area	Diff.	Area	Diff.
Class 1	315.96	307.58	**8.42**	282.67	33.29	204.60	111.40	405.84	89.88	561.29	245.29
Class 2	276.40	284.81	**8.42**	316.15	39.75	326.94	50.55	513.04	236.65	566.87	290.48
Class 3	685.56	679.52	**6.04**	695.37	9.82	743.39	57.80	860.67	175.12	800.88	115.32
Class 4	720.77	726.78	**6.00**	766.26	45.49	806.77	85.99	601.38	119.40	840.48	119.70
Class 5	944.32	965.39	21.06	923.90	**20.42**	985.39	41.07	839.46	104.87	690.01	254.31
Class 6	831.91	810.81	**21.10**	790.53	41.37	707.83	124.08	554.49	277.42	315.35	516.55
Mean			**11.84**		31.69		78.48		167.22		256.94
Std. Dev.			**7.24**		13.84		34.14		76.40		146.68

To assess the performance of the algorithms on the experimental images, we analyzed the results on the basis of several validity indexes. We considered several validity indexes such as the Bezdeks partition coefficient (PC-I) (Bezdek and Pal, 1998), Dunn's separation index (DI), the Davies–Bouldins index (DB-I), the Separation index (S-I), Xie and Benis index (XB-I), and Classification Entropy index (CE-I) (Wang and Zhang, 2007). The validity indexes are reported in Table 4.

Note that the validity indexes are proposed to evaluate the quality of clustering. Algorithms producing better results come with smaller values of T-I, DB-I, XB-I, S-I, CE-I and the larger value of PC-I. The results summarized in Table 4 show that IIT2-FCM or SIIT2-FCM exhibit produce better quality clustering than those obtained when running other commonly encountered algorithms such as IT2FCM, FCM and k-Means, in particular. Visibly, the indexes obtained from SIIT2-FCM are significantly better than those for the IIT2-FCM.

Table 3
Difference (in %) among classes.

Class	SIIT2-FCM	IIT2-FCM	IT2-FCM	FCM	k-Means
1	2.66	10.54	35.26	28.45	77.63
2	3.05	14.38	18.29	85.62	105.09
3	0.88	1.43	8.43	25.54	16.82
4	0.83	6.31	11.93	16.57	16.61
5	2.23	2.16	4.35	11.10	26.93
6	2.54	4.97	14.92	33.35	62.09

5.2. *Land-cover change detection*

The idea for change detection using clustering algorithms is visualized in Fig. 7. In this model, satellite image data at different

Table 4
Validity indexes for the *Landsat7* images of Hanoi region.

Validity index	k-Means	FCM	IT2-FCM	IIT2-FCM	**SIIT2-FCM**
DB-I	4.531	3.4983	2.3981	1.1246	**1.0092**
XB-I	1.761	1.1784	0.6823	0.1382	**0.0986**
S-I	0.9821	0.6287	0.3834	0.0917	**0.0148**
CE-I	1.323	0.9869	0.5872	0.1972	**0.1317**
PC-I	0.6543	0.6982	0.7282	0.8628	**0.8893**

temporal points with 6 bands are input data for the fuzzy classification algorithm. The classification results are compared with individual other to detect the change of land covers. This section presents two experiments of land cover change detection using SIIT2-FCM at four temporal points.

Study case: Data 1 from *Landsat*7 satellite images of Hanoi, Vietnam (20°29′27. 81″N, 106°32′21. 65″E to 21°27′15. 41″N, 104°35′23. 54″E) with area of 3161.304 km^2 at four temporal points in 1995, 200, 2007, and 2009. The resolution of imagery is 30 m × 30 m and the total number of pixels is 3,512,560.

The results of change detection are shown in Fig. 8, in which (a), (b), (c) and (d) are land cover classification at temporal point in 1995, 2000, 2007 and 2009, respectively. Results of the proposed methods are compared with the survey data of the Hanoi Department of Natural Resources and Environment (HDNRE) which are actual data collected by land survey. Fig. 9 shows the change detection of individual class according to temporal points in which Fig. 9(a) is plotted from DNREH data and Fig. 9(b) is obtained from SIIT2-FCM. Tables 5, 6, 7 and 8 show classification results of land covers from multi-spectral satellite imagery of Hanoi at temporal points in 1995, 2000, 2007 and 2009, respectively. The difference between the classified area (in km^2) and DNREH data of individual class, mean and standard deviation obtained from SIIT2-FCM and IIT2-FCM are significantly better than IT2-FCM, FCM and k-Means for all of datasets. For all classes classified from data temporal points, SIIT2-FCM is normally better than IIT2-FCM e.g. in results of 1995-dataset, SIIT2-FCM is better for the classes 1, 2, 3, and 6; in results of 2000-dataset, it is better for the classes 1, 4, and 5; it is better for the classes 1, 2, 5 and 6 in results of 2007-dataset and the classes 1, 4, and 6 in results of 2009-dataset. Especially, the mean and the standard deviation of results obtained from SIIT2-FCM are much better than the ones obtained from IIT2FCM e.g. the standard deviation of 14.91 (1995-dataset), 8.96 (2000-dataset), 15.70 (2007-dataset) and 7.81 (2009-dataset) (SIIT2FCM) are in comparison with 25.91 (1995-dataset), 18.64 (2000-dataset), 41.20 (2007-dataset) and 18.16 (2009-dataset) (IIT2FCM).

In the same way as in the above section, validity indexes consisting of T-I, DB-I, XB-I, S-I, CE-I and PC-I are estimated to evaluate the quality of clustering. Fig. 10 is plotted to compare between different indexes at individual temporal point, in which indexes obtained from SIIT2FCM and IIT2FCM are better than IT2FCM, FCM and k-Means i.e. SIIT2FCM and IIT2FCM led to the better quality of clusters.

Case study: Data 2 from *Landsat*7 satellite images of Bao Loc city, Lam Dong province, Vietnam (11°18′29. 13″N, 108°18′10. 57″E to 11°58′29. 63″N, 107°01′44. 93″E) with the area of 1707.31 km^2 at four temporal points in 1990, 2000, 2010 and 2014. The resolution of imagery is 30 m × 30 m and total of pixels is 1,897,008.

The results of land cover classification for change detection are shown in Fig. 11 in which 11(a), (b), (c) and (d) are land cover classification at temporal points in 1990, 2000, 2010 and 2014, respectively. The captured time of imagery deals with the dry season in South Vietnam, so satellite imagery is not affected by clouds and fog. The results of the proposed algorithms are compared with the survey data of the Lam Dong Department of Natural Resources and Environment (LDNRE) which are actual data of land covers collected by land survey. Fig. 12 shows change detection of individual class according to temporal points in which Fig. 12(a) is from LDNRE data and Fig. 12(b) is from SIIT2-FCM. Tables 9, 10, 11 and 12 show classification results of Bao Loc region at temporal points in 1990, 2000, 2010 and 2014, respectively. The difference of individual class, mean and standard deviation of SIIT2-FCM and IIT2-FCM algorithms is much better than IT2-FCM, FCM and k-Means for all of datasets. Also, SIIT2-FCM is normally better than IIT2-FCM e.g. in results of 1990-dataset, SIIT2-FCM is better for the classes of 1, 5, and 6; in results of 2000-dataset, it is better for the classes 1, 2, 3, 4 and 6; it

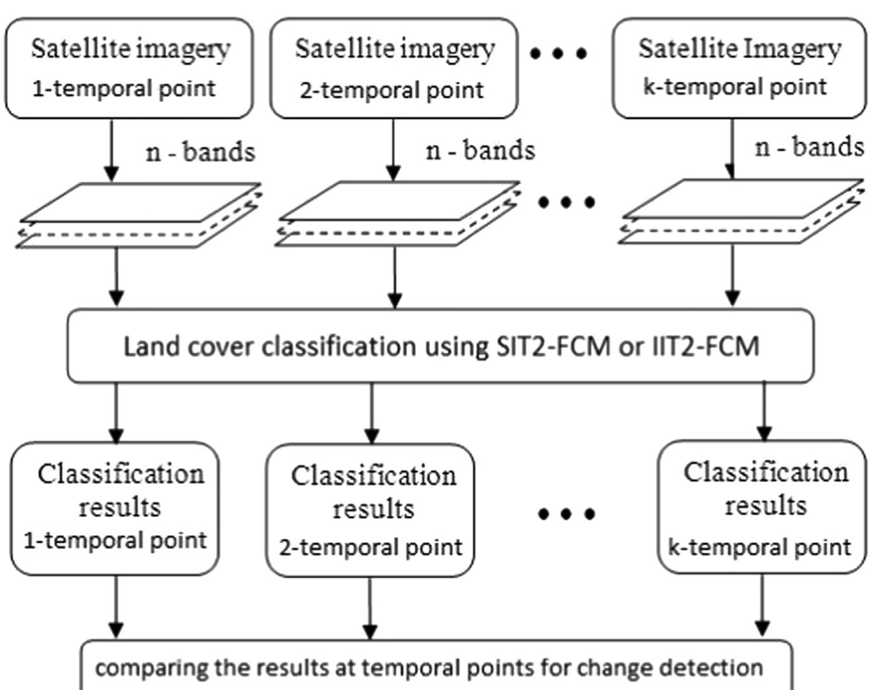

Fig. 7. Model of monitoring land cover changes.

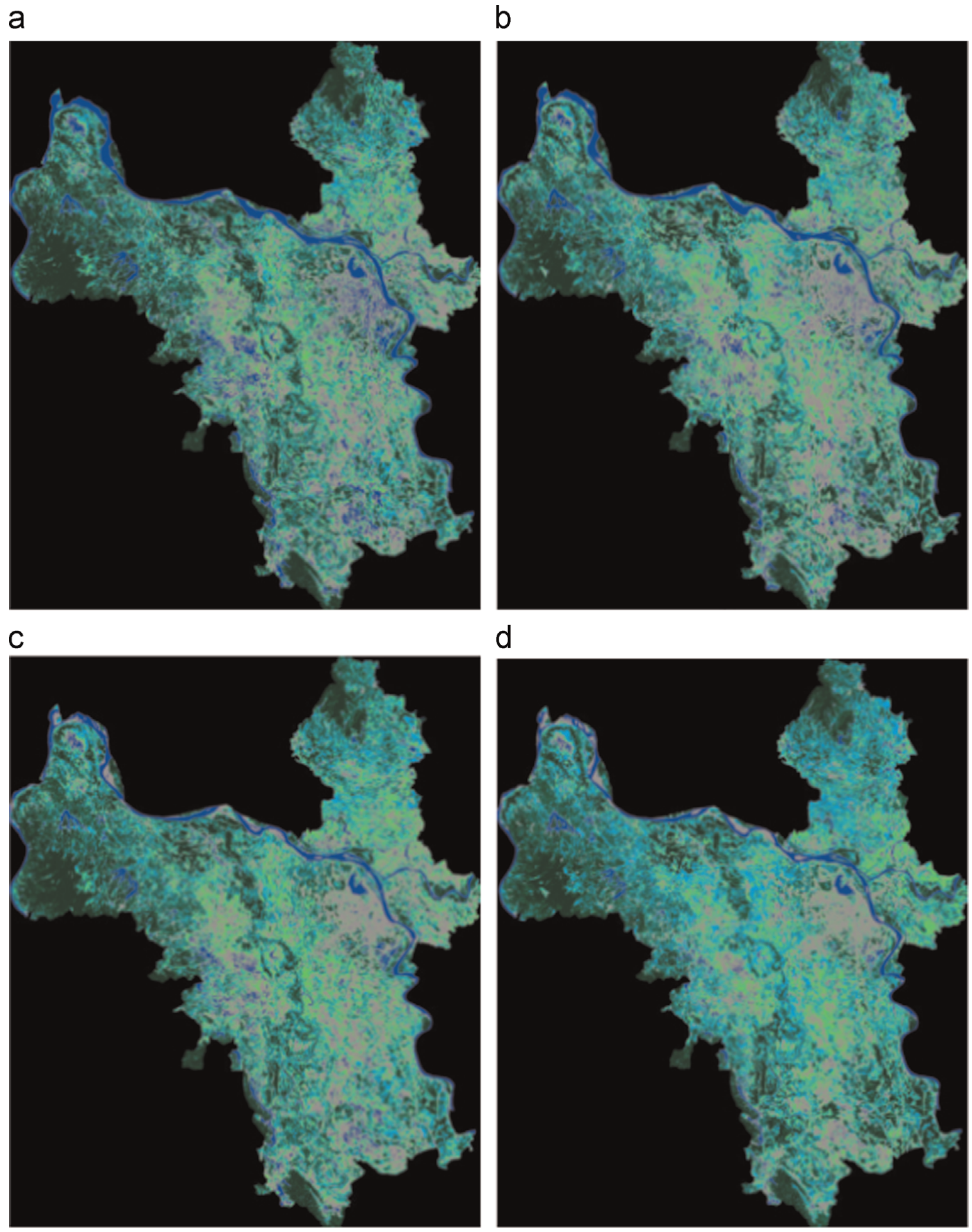

Fig. 8. Change detection of Hanoi region: (a) 1995, (b) 2000, (c) 2007, and (d) 2009.

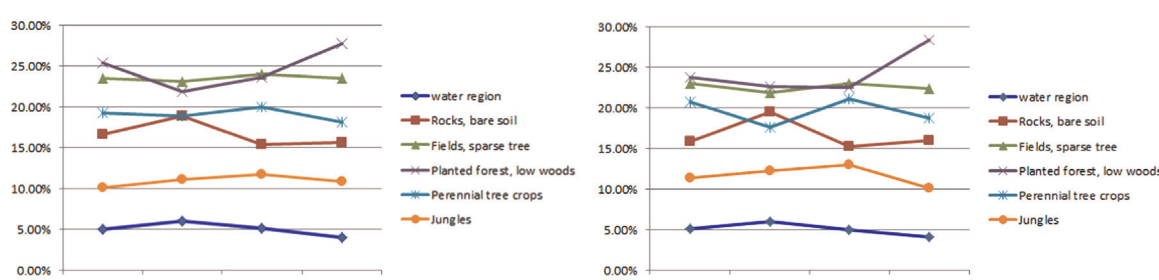

Fig. 9. Change detection of Hanoi region with individual classes. Left: survey data of HDNRE and right: classification by SIIT2FCM.

is better for the classes 1, 4, 5 and 6 in results of 2010-dataset and all classes in results of 2014-dataset. Especially, the mean and the standard deviation obtained from SIIT2-FCM are much better than IIT2FCM e.g. the standard deviation of 9.56 (1990-dataset), 10.90 (2000-dataset), 9.58 (2010-dataset) and 5.13 (2014-dataset) (SIIT2FCM) are in comparison with 13.64 (1990-dataset), 25.35 (2000-dataset), 14.52 (2010-dataset) and 11.10 (2014-dataset) (IIT2FCM). Fig. 13 plots various validity indexes at different temporal points.

In summary, the experiments from two study data pointed out that the boundary of water and soil covers is usually clarified, while the vegetation covers (classes 3, 4, 5, 6) are often confused between them. With satellite image resolution of 30 m × 30 m, the differences of classification results can be acceptable in assessment

Table 5
Land cover classification of the Hanoi region (1995) (km^2).

Class	HDNRE	SIIT2-FCM		IIT2-FCM		IT2-FCM		FCM		k-Means	
	Area	Area	Diff.	Area	Diff.	Area	Diff.	Area	Diff.	Area	Diff.
Class 1	159.84	163.74	**3.89**	164.46	4.62	183.36	23.51	226.47	66.63	289.47	129.62
Class 2	527.04	501.04	**26.00**	491.13	35.91	439.93	87.11	366.21	160.83	321.21	205.83
Class 3	745.27	728.33	**16.94**	762.45	17.18	818.25	72.97	890.23	144.95	935.25	189.97
Class 4	801.58	750.49	51.09	750.75	**50.82**	784.68	16.89	913.40	111.83	994.38	192.81
Class 5	608.60	658.02	49.41	603.85	**4.76**	532.02	76.58	496.02	112.58	406.02	202.58
Class 6	318.96	359.69	**40.73**	388.66	69.69	403.07	84.10	268.97	50.00	214.97	104.00
Mean			36.84		**35.67**		67.53		116.04		179.04
Std. Dev.			**14.91**		25.91		28.87		42.52		42.46

Table 6
Land cover classification of the Hanoi region (2000) (km^2).

Class	HDNRE	SIIT2-FCM		IIT2-FCM		IT2-FCM		FCM		k-Means	
	Area	Area	Diff.	Area	Diff.	Area	Diff.	Area	Diff.	Area	Diff.
Class 1	189.86	**189.89**	**0.03**	188.74	1.12	226.47	36.61	289.48	99.62	335.81	145.95
Class 2	598.02	617.16	19.14	**616.35**	**18.32**	573.21	24.81	528.21	69.81	443.57	154.45
Class 3	731.18	692.70	38.47	**708.45**	**22.73**	728.23	2.95	746.25	15.07	756.16	24.99
Class 4	692.48	**717.73**	**25.25**	739.68	47.21	814.40	121.93	895.39	202.91	1031.70	339.22
Class 5	596.84	**556.74**	**40.10**	541.02	55.82	523.02	73.82	469.02	127.82	381.45	215.39
Class 6	352.93	387.08	34.15	**367.07**	**14.14**	295.97	56.96	232.95	119.97	212.60	140.32
Mean			**31.42**		31.64		56.09		107.12		174.87
Std. Dev.			**8.96**		18.64		45.97		70.06		114.81

Table 7
Land cover classification of the Hanoi region (2007) (km^2).

Class	HDNRE	SIIT2-FCM		IIT2-FCM		IT2-FCM		FCM		k-Means	
	Area	Area	Diff.	Area	Diff.	Area	Diff.	Area	Diff.	Area	Diff.
Class 1	161.87	**160.05**	**1.82**	163.78	1.90	185.97	24.10	230.25	68.38	245.82	83.94
Class 2	485.03	**483.88**	**1.16**	471.64	13.39	420.88	64.16	368.48	116.55	272.57	212.46
Class 3	761.18	727.38	33.80	**747.44**	**13.73**	872.28	111.10	918.02	156.84	1017.17	255.99
Class 4	748.48	711.92	36.56	**724.98**	**23.50**	766.10	17.62	933.86	185.38	995.71	247.23
Class 5	632.84	**666.93**	**34.09**	572.40	60.44	513.93	118.91	409.48	223.36	381.46	251.39
Class 6	371.93	**411.17**	**39.25**	481.09	109.16	402.17	30.25	301.23	70.69	248.60	123.32
Mean			**28.97**		44.05		68.41		150.57		218.08
Std. Dev.			**15.70**		41.20		45.90		59.35		55.69

Table 8
Land cover classification of the Hanoi region (2009) (km^2).

Class	HDNRE	SIIT2-FCM		IIT2-FCM		IT2-FCM		FCM		k-Means	
	Area	Area	Diff.	Area	Diff.	Area	Diff.	Area	Diff.	Area	Diff.
Class 1	128.24	**130.92**	**2.69**	141.58	13.34	163.77	35.54	212.25	84.01	246.71	118.48
Class 2	494.60	508.11	13.52	**499.62**	**5.03**	462.63	31.96	449.48	45.12	396.77	97.83
Class 3	743.79	708.68	35.11	**723.16**	**20.63**	837.44	93.65	891.01	147.23	945.16	201.38
Class 4	878.33	**899.03**	**20.71**	833.46	44.87	787.98	90.35	843.85	34.47	1013.70	135.37
Class 5	573.86	595.47	21.61	581.40	**7.53**	482.40	91.47	373.48	200.38	273.45	300.41
Class 6	342.50	**319.09**	**23.41**	382.09	39.59	427.09	84.59	391.23	48.73	285.50	56.99
Mean			**22.87**		23.53		78.40		95.19		158.40
Std. Dev.			**7.81**		18.16		26.18		74.37		95.52

of land cover on a large area quickly and reduce costs compared to other ways of change detection. This result not only makes predictions about the land cover fluctuations but could also help support planning urban, natural resources management, etc.

6. Conclusions

In this study, we have presented two fuzzy clustering algorithms based on interval type-2 Fuzzy C-Means. The first one is based on a combination of IT2-FCM when using some spatial relationships between the pixels and their neighbors. The second one uses the set of pre-determined centroids. The advantages of the proposed algorithms are pointed out in the context of two applications to land cover classification and the change detection. Experiments are completed for two datasets of Hanoi and Bao Loc (Vietnam) produced via *Landsat7* multi-spectral imagery. We showed the efficiency of the approach in monitoring the changes of land cover and the change of environment. The developed

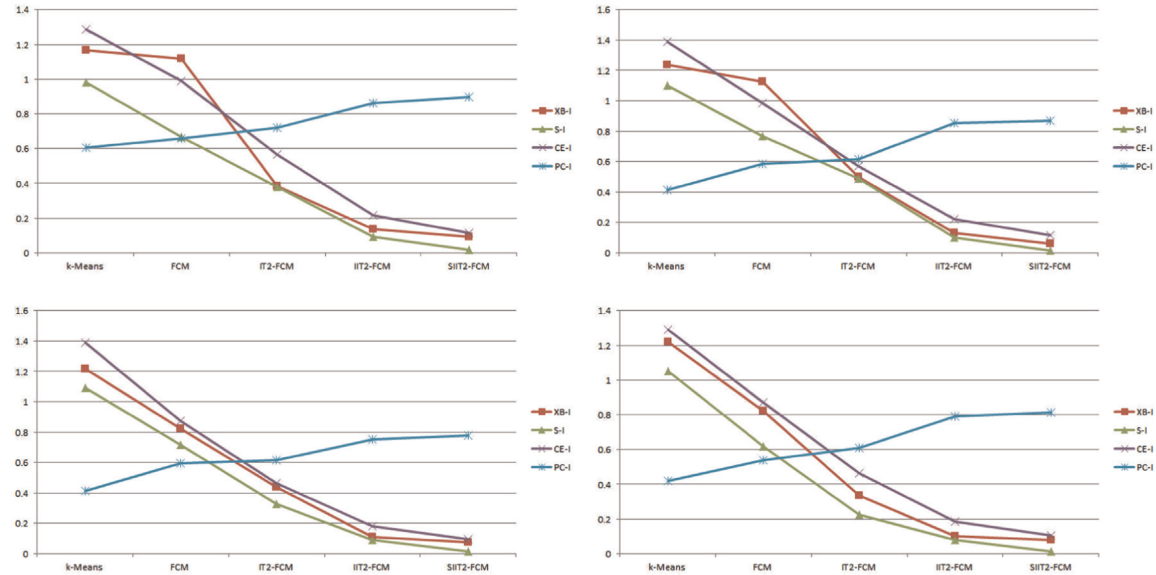

Fig. 10. Validity indexes of Hanoi's land cover classification at temporal points: top-left: 1995, top-right: 2000, bottom-left: 2007 and bottom-right: 2009.

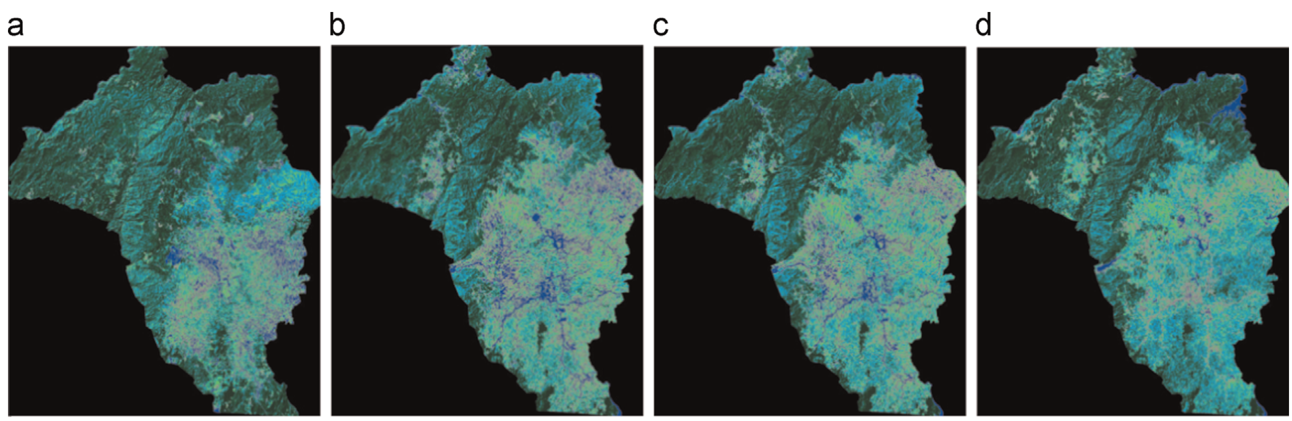

Fig. 11. Change detection of Bao Loc with individual class.

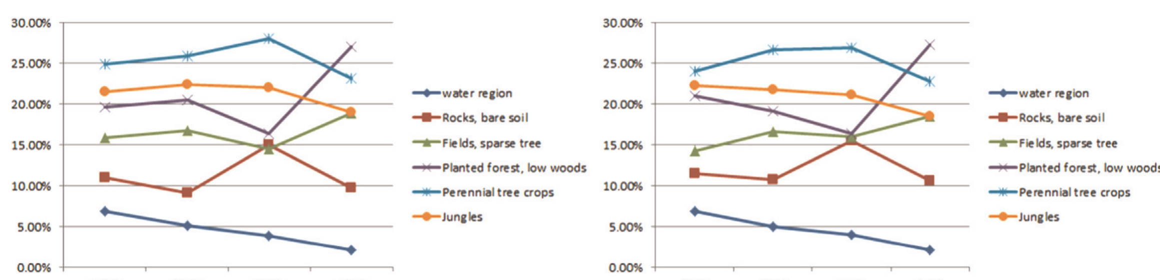

Fig. 12. Change detection of Bao Loc with individual classes. Top: survey data of LDNRE and bottom: classification by SIIT2FCM.

Table 9
Land cover classification of Bao Loc (1990) (km^2).

Class	LDNRE	SIIT2-FCM		IIT2-FCM		IT2-FCM		FCM		k-Means	
	Area	Area	Diff.	Area	Diff.	Area	Diff.	Area	Diff.	Area	Diff.
Class 1	118.64	116.97	**1.66**	114.72	3.91	110.22	8.41	101.22	17.41	90.42	28.21
Class 2	187.49	196.31	8.82	193.79	**6.30**	187.49	0.00	178.49	9.00	133.49	54.00
Class 3	271.32	244.05	27.27	253.32	**18.00**	289.32	18.00	316.32	45.00	343.32	72.00
Class 4	335.14	359.16	24.02	324.06	**11.08**	333.06	2.08	338.46	3.32	360.06	24.92
Class 5	426.20	410.12	**16.08**	467.90	41.70	482.30	56.10	536.30	110.10	599.30	173.10
Class 6	368.51	380.69	**12.18**	353.51	15.00	304.91	63.60	236.51	132.00	180.71	187.80
Mean			**15.00**		16.00		24.70		52.81		90.01
Std. Dev.			**9.56**		13.64		28.04		55.20		72.31

Table 10
Land cover classification of Bao Loc (2000) (km^2).

Class	LDNRE	SIIT2-FCM		IIT2-FCM		IT2-FCM		FCM		k-Means	
	Area	Area	Diff.	Area	Diff.	Area	Diff.	Area	Diff.	Area	Diff.
Class 1	86.889	85.95	**0.94**	87.93	1.04	88.72	1.83	89.52	2.63	115.62	28.73
Class 2	157.129	184.93	**27.81**	226.15	69.03	290.16	133.03	349.49	192.36	385.49	228.36
Class 3	286.213	283.74	**2.48**	270.23	15.98	261.23	24.98	226.32	59.89	181.32	104.89
Class 4	350.47	326.79	**23.68**	316.89	33.58	298.89	51.58	270.07	80.40	252.07	98.40
Class 5	443.181	454.40	11.22	440.90	**2.28**	468.80	25.62	500.30	57.12	518.30	75.12
Class 6	383.437	371.51	**11.93**	365.21	18.23	299.51	83.93	271.61	111.83	254.51	128.93
Mean			**13.01**		23.35		53.50		84.04		110.74
Std. Dev.			**10.90**		25.35		47.99		63.96		66.85

Table 11
Land cover classification of Bao Loc (2010) (km^2).

Class	LDNRE	SIIT2-FCM		IIT2-FCM		IT2-FCM		FCM		k-Means	
	Area	Area	Diff.	Area	Diff.	Area	Diff.	Area	Diff.	Area	Diff.
Class 1	66.59	68.68	**2.09**	72.85	6.26	79.81	13.22	89.88	23.29	116.52	49.93
Class 2	257.34	265.42	8.08	252.59	**4.75**	227.07	30.27	196.49	60.85	177.59	79.75
Class 3	248.73	272.86	24.13	261.94	**13.21**	234.23	14.50	225.96	22.77	199.32	49.41
Class 4	279.36	279.17	**0.19**	280.75	1.39	262.89	16.48	225.06	54.30	180.06	99.30
Class 5	479.25	460.05	**19.20**	439.55	39.70	459.80	19.45	509.30	30.05	536.30	57.05
Class 6	376.03	361.12	**14.91**	399.62	23.59	443.51	67.48	460.61	84.58	497.51	121.48
Mean			**11.43**		14.82		26.90		45.97		76.15
Std. Dev.			**9.58**		14.52		20.80		24.85		29.57

Table 12
Land cover classification of Bao Loc (2014) (km^2).

Class	LDNRE	SIIT2-FCM		IIT2-FCM		IT2-FCM		FCM		k-Means	
	Area	Area	Diff.	Area	Diff.	Area	Diff.	Area	Diff.	Area	Diff.
Class 1	35.71	36.57	**0.86**	36.75	1.04	43.05	7.34	46.51	10.80	67.69	31.99
Class 2	166.46	182.80	**16.34**	189.81	23.35	214.11	47.65	183.75	17.29	140.32	26.14
Class 3	322.61	315.60	**7.01**	344.40	21.79	317.40	5.21	268.70	53.91	209.95	112.65
Class 4	461.61	466.71	**5.11**	430.71	30.89	421.71	39.89	493.88	32.27	567.17	105.57
Class 5	396.32	390.02	**6.30**	405.32	9.00	426.02	29.70	488.86	92.54	541.04	144.72
Class 6	324.61	315.61	**8.99**	300.32	24.29	285.02	39.59	225.62	98.99	181.12	143.48
Mean			**7.44**		18.40		28.23		50.97		94.09
Std. Dev.			**5.13**		11.10		17.95		37.79		52.83

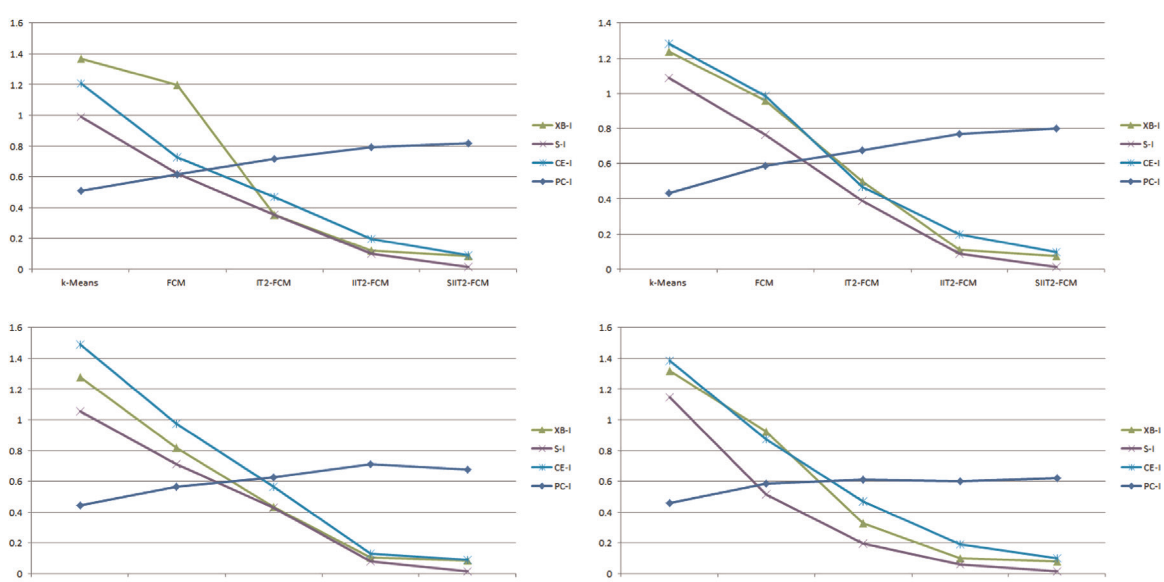

Fig. 13. The validity indexes of algorithms on Bao Loc data. Top-left: 1990, top-right: 2000, bottom-left: 2010, and bottom-right: 2014.

clustering methods may be applied to other applications including planning urban and forestry management, among others.

There are several further research directions including the use and refinement of the proposed clustering to processing hyperspectral satellite images with application to environmental classification and assessment of land surface temperature changes. The issues of speed-ups of the proposed methods based on GPU platforms form another important research direction.

References

Benaichouche, A.N., Oulhadj, H., Siarry, P., 2013. Improved spatial fuzzy C-means clustering for image segmentation using PSO initialization, Mahalanobis distance and post-segmentation correction. Digit. Signal Process. 23, 1390–1400.

Bezdek, J.C., Pal, N., 1998. Some new indexes of cluster validity. IEEE Trans. Syst. Man Cybern. 28 (3), 301–315.

Bezdek, J.C., Ehrlich, R., Full, W., 1984. FCM: the fuzzy C-means clustering algorithm. Comput. Geosci. 10 (2–3), 191–203.

Despotovic, I., Goossens, B., Vansteenkiste, E., Philips, W., 2010. An improved fuzzy clustering approach for image segmentation. In: The 17th IEEE International Conference on Image Processing, pp. 249–252.

Fisher, P.F., 2010. Remote sensing of land cover classes as type 2 fuzzy sets. Remote Sens. Environ. 114, 309–321.

Ghaffarian, S., Ghaffarian, S., 2014. Automatic histogram-based fuzzy C-means clustering for remote sensing imagery. ISPRS J. Photogramm. Remote Sens. 97, 46–57.

Ghosha, S., Roy, M., Ghosh, A., 2014. Semi-supervised change detection using modified self-organizing feature map neural network. Applied Soft Comput. 15, 1–20.

Ghosh, A., Mishra, N.S., Ghosh, S., 2011. Fuzzy clustering algorithms for unsupervised change detection in remote sensing images. Inf. Sci. 181, 699–715.

Hwang, C., Rhee, F.C.H., 2007. Uncertain fuzzy clustering: interval Type-2 fuzzy approach to C-Means. IEEE Trans. Fuzzy Syst. 15 (1), 107–120.

Ji, Z., Xia, Y., Sun, Q., Cao, G., 2014. Interval-valued possibilistic fuzzy C-means clustering algorithm. Fuzzy Sets Syst. 253, 138–156.

Karnik, N., Mendel, J.M., 2001. Centroid of a type-2 fuzzy set. Inf. Sci. 132, 195–220.

Karnik, N., Mendel, J.M., Liang, Q., 1999. Type-2 fuzzy logic systems. IEEE Trans. Fuzzy Syst. 7 (6), 643–658.

Liang, Q., Mendel, J.M., 2000. Interval type-2 fuzzy logic systems: theory and design. IEEE Trans. Fuzzy Sys., 535–550.

Liu, F., 2008. An efficient centroid type-reduction strategy for general type-2 fuzzy logic system. Inf. Sci. 178 (9), 2224–2236.

Liu, J., Pham, T.D., 2012. A spatially constrained fuzzy hyper-prototype clustering algorithm. Pattern Recognit. 45, 1759–1771.

Liu, H., Zhao, F., Jiao, L., 2012. Fuzzy spectral clustering with robust spatial information for image segmentation. Appl. Soft Comput. 12, 3636–3647.

Liu, Y., Zhang, B., Wang, L., Wang, N., 2013. A self-trained semisupervised SVM approach to the remote sensing land cover classification. Comput. Geosci. 59, 98–107.

Martinez, V.F., Martinez, E.F., 2014. Spectral clustering for sensing urban land use using Twitter activity. Eng. Appl. Artif. Intell. 35, 237–245.

Mendel, J.M., John, R.I., 2002. Type-2 fuzzy sets made simple. IEEE Trans. Fuzzy Syst. 10 (2), 117–127.

Mendel, J.M., John, R.I., Liu, F., 2006. Interval Type-2 fuzzy logic systems made simple. IEEE Trans. Fuzzy Syst. 14 (6), 808–821.

Mishra, N.S., Ghosh, S., Ghosh, A., 2012. Fuzzy clustering algorithms incorporating local information for change detection in remotely sensed images. Appl. Soft Comput. 12, 2683–2692.

Ngo, L.T., Nguyen, D.D., 2012. Land cover classification using interval type-2 fuzzy clustering for multi-spectral satellite imagery. In: IEEE Conference on SMC, pp. 2371–2376.

Nguyen, D.D., Ngo, L.T., Pham, L.T., Pedrycz, W., Towards hybrid clustering approach to data classification: multiple kernel based-interval-valued fuzzy C-means algorithms. Fuzzy Sets Syst. (2015), http://dx.doi.org/10.1016/j.fss.2015.01.020.

Qiu, C., Xiao, J., Yu, L., Han, L., Iqbal, M.N., 2013. A modified interval type-2 fuzzy C-means algorithm with application in MR image segmentation. Pattern Recognit. Lett. 34, 1329–1338.

Roy, M., Ghosh, S., Ghosh, A., 2014. A novel approach for change detection of remotely sensed images using semi-supervised multiple classifier system. Inf. Sci. 269, 35–47.

Shankar, B.U., Meher, S.K., Ghosh, A., 2011. Wavelet-fuzzy hybridization: feature-extraction and land-cover classification of remote sensing images. Appl. Soft Comput. 11, 2999–3011.

Stavrakoudis, D.G., Theocharis, J.B., Zalidis, G.C., 2011. A boosted genetic fuzzy classifier for land cover classification of remote sensing imagery. ISPRS J. Photogramm. Remote Sens. 66, 529–544.

Torshizi, A.D., Zarandi, M.H.F., 2014a. A new cluster validity measure based on general type-2 fuzzy sets: application in gene expression data clustering. Knowl.-Based Syst. 64, 81–93.

Torshizi, A.D., Zarandi, M.H.F., Alpha-plane based automatic general type-2 fuzzy clustering based on simulated annealing meta-heuristic algorithm for analyzing gene expression data. Computers in Biology and Medicine (2014b), http://dx.doi.org/10.1016/j.compbiomed.2014.06.017.

Vargas, D.M., Funes, F.J.G., Silva, A.J.R., 2013. A fuzzy clustering algorithm with spatial robust estimation constraint for noisy color image segmentation. Pattern Recognit. Lett. 34, 400–413.

Wang, Z.M., Soha, Y.C., Songa, Q., Sim, K., 2009. Adaptive spatial information-theoretic clustering for image segmentation. Pattern Recognit. 42, 2029–2044.

Wang, W., Zhang, Y., 2007. On fuzzy cluster validity indices. Fuzzy Sets Syst. 158, 2095–2117.

Wang, Z., Song, Q., Soh, Y.C., Sim, K., 2013. An adaptive spatial information-theoretic fuzzy clustering algorithm for image segmentation. Comput. Vis. Image Underst. 117, 1412–1420.

Yuan, Y., Ly, H., Lu, X., 2015. Semi-supervised change detection method for multi-temporal hyperspectral images. Neurocomputing 148, 363–375.

Zarinbal, M., Zarandi, M.H.F., Turksen, I.B., 2014. Interval type-2 relative entropy fuzzy C-means clustering. Inf. Sci. 272, 49–72.

Zhao, F., 2013. Fuzzy clustering algorithms with self-tuning non-local spatial information for image segmentation. Neurocomputing 106, 115–125.

Zhao, F., Jiao, L., Liu, H., Gao, X., 2011. A novel fuzzy clustering algorithm with non local adaptive spatial constraint for image segmentation. Signal Process. 91, 988–999.

Zhao, F., Jiao, L., Liu, H., 2013. Kernel generalized fuzzy C-means clustering with spatial information for image segmentation. Digit. Signal Process. 23, 184–199.